



# Leveraging Transfer Learning for Rapid Adaptation of ML-based Indoor Propagation Models

Melina Geis, Nicolas Faust, Hendrik Schippers, Stefan Böcker, and Christian Wietfeld

Communication Networks Institute, TU Dortmund University, 44227 Dortmund, Germany

e-mail: {Melina.Geis, Nicolas.Faust, Hendrik.Schippers, Stefan.Boecker, Christian.Wietfeld}@tu-dortmund.de

**Abstract**—Adaptive 6G networks are crucial for maintaining reliable communication in dynamically changing environments. To this end, accurate propagation models are essential for network adaptation, but developing real-time, high-fidelity models is a significant challenge. Machine Learning (ML)-based channel models have gained attention in recent years, yet their limited generalizability often necessitates extensive retraining to ensure applicability in unseen environments. In this paper, we propose a process chain for rapid network adaptation in dynamic environments. Our fully automated process encompasses network Key Performance Indicator collection, LiDAR-based environmental modeling, Transfer Learning (TL)-assisted refinement of the ML-based IndoorDRaGon propagation model, and network planning. We demonstrate that Artificial Neural Networks (ANNs) achieve comparable accuracy to Random Forest (RF)-based models while offering significantly faster adaptation to new environments. Unlike RFs, ANNs do not need to be retrained from scratch using all the source data, which reduces computational effort and improves data privacy as only the new data is required. This enables efficient and dynamic network reconfiguration in previously unseen scenarios with just a few new measurements.

## I. INTRODUCTION

5G and future 6G network infrastructures are critical for enabling seamless operations and efficient communication in complex industrial and logistics environments. These networks need to provide the high-speed, low-latency, and ultra-reliable connectivity required for real-time operations and the increasing number of connected industrial devices. However, such environments are highly dynamic - moving machinery, reconfigured layouts, and fluctuating inventory levels continuously alter radio propagation characteristics. As a result, areas with previously strong network coverage may experience degraded connectivity, requiring continuous network reconfiguration to maintain optimal performance. To address these challenges, network planning and channel modeling must be highly adaptive and scalable, capable of responding rapidly to environmental changes. Existing approaches either lack the necessary precision or are too computationally intensive for real-time application. Machine Learning (ML)-driven methods have emerged as a promising solution, enabling rapid and accurate modeling.

Fig. 1 illustrates an intralogistics use case where rapid environmental changes contrast with a static communication network. In this paper, we present a methodology for rapidly and accurately adapting the network to new situations in unknown and dynamic environments. Our approach builds upon our previously presented ML-driven indoor propagation

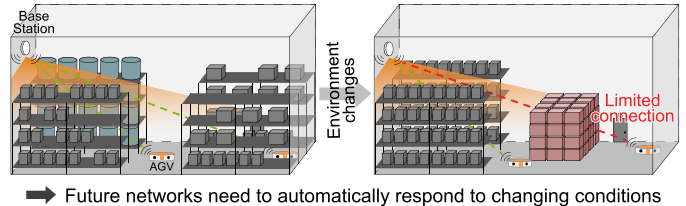


Fig. 1. Dynamic environments place high demands on local wireless networks, requiring adaptive reconfiguration to maintain performance, as static networks fail to respond effectively to changing conditions

model, IndoorDRaGon [1], for optimizing Base Station (BS) positions and rapid ML model adaptation by leveraging fine-tuning, a Transfer Learning (TL) approach.

The remainder of the paper is structured as follows. After discussing the related work in Sec. II, the proposed approach for network optimization and rapid model adaptation is presented in Sec. III. Methodological aspects are outlined in Sec. IV, and followed by detailed results in Sec. V.

## II. RELATED WORK

A wide range of channel models is available, partly designed especially for indoor scenarios. Empirical models, such as those presented by 3GPP in [2], are often used because of their ease of implementation and computational efficiency. However, in many cases, these models do not perform well in unknown, novel scenarios. Ray tracing methods [3] can provide a remedy, but their prediction accuracy is highly dependent on the level of detail of the environmental model, which is typically absent for indoor scenarios. In addition, ray tracing computations are time-consuming and require high computing resources [4].

Several ML-based channel models have been published in recent years, often outperforming empirical models in accuracy [5]. [6] provides a comprehensive review of ML techniques for radio wave propagation modeling, outlining key challenges and examining indoor and outdoor models from the literature. Most ML-based indoor propagation models are trained and tested within the same environment, leaving their generalizability to unseen scenarios largely unexamined. Designing a model that performs well across indoor environments remains a significant challenge. Additionally, most ML-driven channel models rely on offline training, requiring full retraining when new data becomes available. A further challenge is the availability of sufficient measurement data. In [7], this issue is addressed by using a small amount of

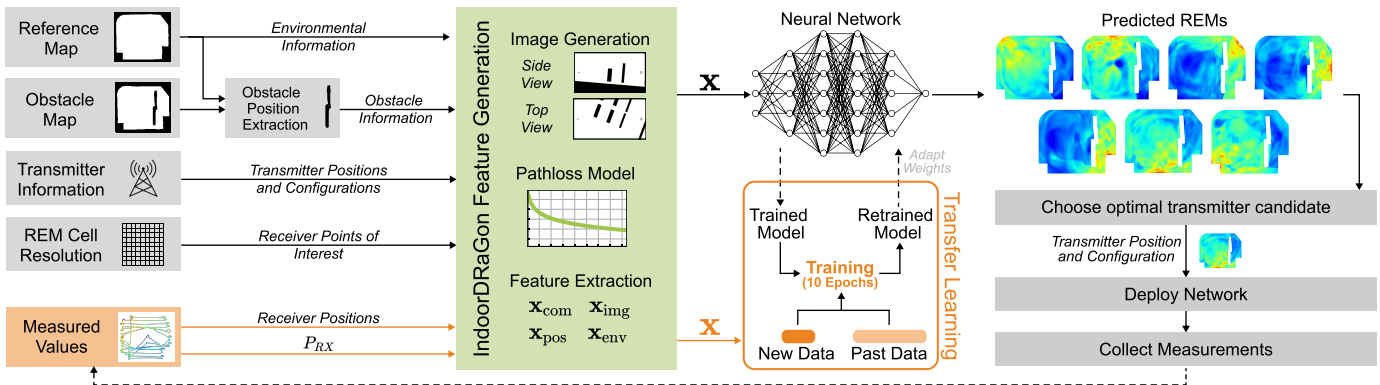


Fig. 2. Overall architecture of the network optimization and Transfer Learning-assisted ML model adaptation process

measurement data to calibrate ray tracing software, which is then utilized to generate synthetic data. Other approaches, such as [8], rely solely on uncalibrated synthetic data, potentially limiting model accuracy in real-world applications.

TL has emerged as a promising solution to this challenge, offering reduced computation time and energy consumption. In [9], TL is applied to adapt an outdoor channel prediction Convolutional Neural Network (CNN) to a new environment. TL has also been used for indoor radio map estimation, as carried out in [10], where modified environments are generated by changing the object's position. [11] addresses the challenge of sparse measurements by initially training a CNN-based indoor propagation model on synthetic data and later refining it with a small set of measurements to reduce ray tracing-induced approximation errors. The authors in [12] utilize TL to adapt their pretrained CNN model to new frequencies. *Online training* is another way to adapt models when little new data is available. This enables incremental updates as new data becomes available, which allows for a rapid adaptation to changing channel conditions. In [13], online training is applied for channel estimation in Orthogonal Frequency-Division Multiplexing (OFDM) systems, while [14] presents a framework for real-time propagation environment modeling and signal strength prediction.

### III. PROPOSED INDOOR NETWORK OPTIMIZATION

**Problem Statement:** We want to design a process chain in which the BS location is optimized for an unknown obstacle constellation but known hall environment. Fig. 2 shows the overall system architecture of the proposed network optimization approach, which consists of mainly two parts: accurate indoor propagation modeling and a network planning stage. Furthermore, this process chain incorporates the possibility of rapidly adapting the propagation model as new data emerges, ensuring continuous optimization in dynamic environments.

**Channel Modeling:** The propagation modeling, which constitutes the basis for network planning, is conducted utilizing the IndoorDRaGoN method, which we presented in [1]. IndoorDRaGoN is a lightweight ML-based path loss prediction method, that uses a Random Forest (RF) for predicting the path loss given 29 numerical features. Thereby, IndoorDRaGoN relies on features extracted from two environmental

images describing the direct path between transmitter and receiver. Further information is provided in Sec. IV. Since IndoorDRaGoN was trained for a specific indoor environment, reference measurements of a new environment must first be taken in order to adapt it to the new environment. For the subsequent network planning step, it is also essential that planning is carried out as quickly and resource-efficiently as possible in order to avoid delays during operation in industrial applications. However, RFs need to be retrained from scratch as they do not allow for concepts like TL or online learning. Hence, we consider an Artificial Neural Network (ANN)-based IndoorDRaGoN variant to allow rapid adaptation to new data.

**Transmitter Placement:** IndoorDRaGoN is used to determine the coverage map for a possible transmitter position and configuration. Solely using a scenario map, a transmitter specification, and a Radio Environmental Map (REM) cell resolution determining possible receiver positions, the required features for the ML predictor can be extracted and used for predictions. In practice, the installation of BSs is not possible in arbitrary locations. Consequently, the potential transmitter locations are predefined, resulting in a finite solution space. Note that while any number of BSs can be considered, the computational complexity increases linearly with each additional position.

### IV. DATA ACQUISITION, PREPROCESSING, AND USAGE

**Data collection:** Compared to *environment 1* [1], where a cable robot was utilized in order to collect 3D measurements, we use an agile ground robot, see Fig. 3a, in this work. It is based on the *DJI Robomaster* platform featuring Omni wheels, allowing the robot to move quickly to any position and orientation. For reliable localization, we utilized Simultaneous Localization and Mapping (SLAM) based on Light Detection and Ranging (LiDAR) and Inertial Measurement Unit (IMU) data. All devices are connected to a System-on-a-Chip (SoC) running *ROS2*. This device simultaneously orchestrates and measures 5G connectivity. A 5G modem with four vertically oriented rod antennas with a peak gain of 2.2 dBi is connected to the SoC. For consistent signal strength measurements, a fixed orientation of the antennas is guaranteed by automating navigation to a grid of predefined measurement points with a fixed goal orientation using *NAV2* [15].



(a) Mobile robot with 5G modem (b) Measurement setup for scenario F  
Fig. 3. Measurement data collection and playground of environment 2

In a first step, the scenario is traversed by teleoperating the robot to create a scenario obstacle map using SLAM. Based on the resulting map, the robot can automatically drive along the scenario grid-wise, thus enabling systematic surveying of network Key Performance Indicators (KPIs). The folding displays from [1] are reused as obstacles for collecting measurements in the new, unknown *environment 2*. We defined eight distinct scenarios for training data collection in order to retrain the IndoorDRaGon model on the new measurement environment (see Fig. 4 Scenario A-H). Thereby, the scenarios are designed as distinct as possible. The environment is limited to a fixed playground with a size of roughly  $8.5 \times 7.0$  m. For each training scenario, we performed the measuring process for seven BS positions (cf. Fig. 4 Scenario A): At each of the four corners of the playground and in the middle of the sides of the playground, with the exception of the left-hand side. An image of Scenario F is shown in Fig. 3b with the BS located at position 7. The BS is always oriented towards the playground, mounted at a height of 1.84 m, using a center frequency of 3725 MHz, 50 MHz of bandwidth, 30 kHz subcarrier spacing, TDD pattern 5:5, and 0 dBm transmission power.

In total, 100K measurement points are collected. Fig. 5 shows the measured Reference Signal Received Power (RSRP) in the empty hall scenario conducted in [1] and the new data recorded in this work. As becomes evident, the trend the data follows differs between the two hall environments. While the data conducted in this work is relatively similar to the freespace path loss, the original IndoorDRaGon data follows a significantly flatter trend for larger propagation distances.

**Data preprocessing:** In comparison to [1], where a complex

digital twin of the environment was used to render sectional images of the scenario, the top and side view images are generated geometrically here without graphical interface allowing for a more resource efficient feature extraction. This enables the circumvention of a complex digital twin, with the environment model instead being generated from the SLAM map. While the top view images can be created from the determined obstacle map by selecting the image section based on the position of the transmitter and receiver analogous to [1], the positions of the obstacles must be determined for the generation of the side view images. To distinguish between dynamically changing objects and fixed environmental components, the static environment is surveyed in a first step so that the non-static objects can be detected by superimposing newly recorded scenarios with the reference map (cf. Fig. 2). The objects can subsequently be extracted by edge detection and assigned a height. With known transmitter and receiver positions (localization via SLAM), side view images and intersections with obstacles can be computed. Similar to [1] the amount of black pixels for three horizontal and five vertical split sections are extracted for both synthetic image types. The considered feature domains and explicit 27 features are listed in Tab. I. Compared to [1], three communication-aware features are removed because they do not change between scenarios, while the distance to the first intersection is added.

TABLE I  
LOGICAL SUBVECTORS OF UTILIZED ML FEATURE VECTOR.

Subvector	Features
$\mathbf{x}_{\text{com}}$	Estimated path loss $L$
$\mathbf{x}_{\text{pos}}$	Position differences $\Delta x$ , $\Delta y$ , $\Delta z$ , deviation from main antenna beam $\Delta\theta$ , $\Delta\varphi$ , 3D distance $d_{3D}$ , receiver height $z$
$\mathbf{x}_{\text{img}}$	Relation of obstacle pixels for three horizontal and five vertical split sections for top-view ( $\mathbf{x}_{\text{top}}$ ) and side-view ( $\mathbf{x}_{\text{side}}$ ) images
$\mathbf{x}_{\text{env}}$	oLOS distance $d_{\text{OLOS}}$ , number of intersections $N_{\text{IS}}$ , distance to first intersection $d_{\text{IS}}$

**Transfer Learning:** In [1], the IndoorDRaGon model is trained once on the training data. However, as soon as new measurement data becomes available, it is beneficial to utilize it for the ML model, thereby enhancing its generalization. As ANNs allow for iterative learning, we employ fine-tuning, a

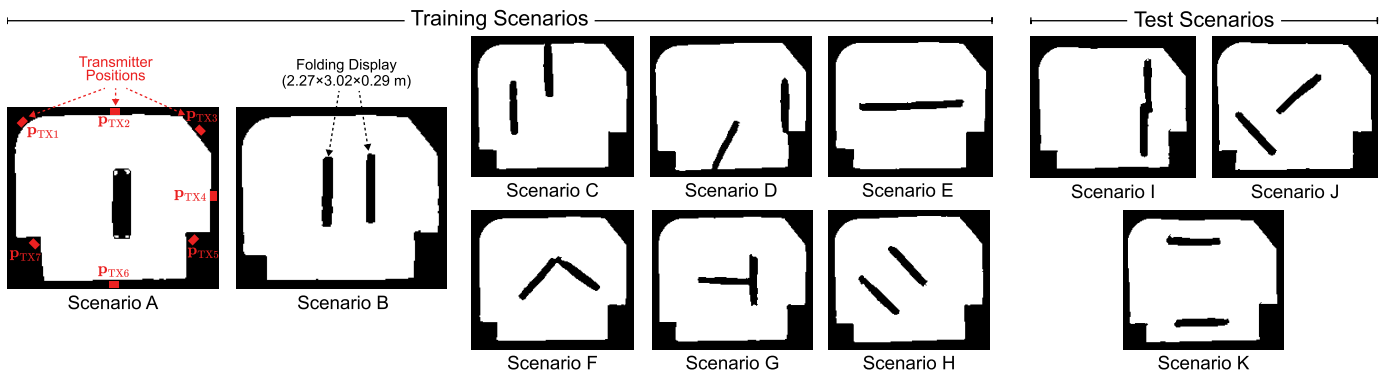


Fig. 4. LiDAR scans of the measurement scenarios in environment 2 from top-view perspective

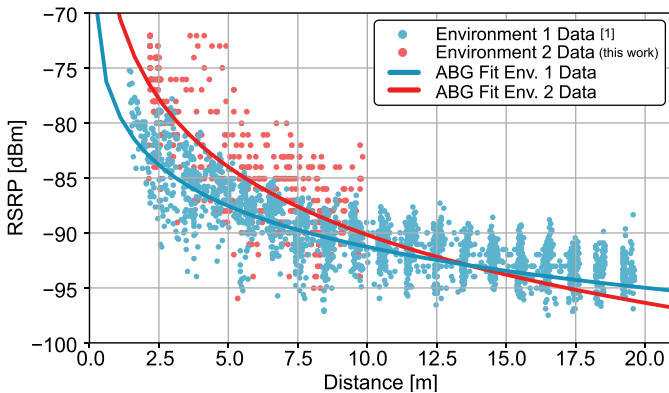


Fig. 5. Comparison of the hall propagation characteristics: Measured RSRP taken in the empty hall environments over the distance

TL type, to efficiently adapt an already trained model to new, unseen scenarios. This is achieved by training the ANN for additional epochs leveraging the new data.

**Network Planning:** To realize network optimization for a new environment, a map of the modified scenario and a defined BS solution space are required. Consequently, IndoorDRaGon is used to generate a REM for each BS position of interest (cf. Fig. 2). From the resulting solution space, the best BS is selected by maximizing the mean received power  $P_{RX}$ .

## V. EVALUATION, EXPLOITATION, AND OPTIMIZATION OF ML-BASED PROPAGATION MODELING

### A. Adaptation to New Hall Environment

As already pointed out, the propagation characteristics of the hall environment in [1] differ from the one in this work. It can be inferred that the model trained in [1] lacks transferability to the new environment. In order to verify this hypothesis, the ML model is trained and tested on different combinations of data: original data only, new data only, and both data combined. The performance of the model on the corresponding hold-out test data is illustrated in Fig. 6. Notably, the transferability is not given for both directions, resulting in more than doubled Root Mean Squared Error (RMSE) values. However, training the RF on the aggregated data leads to enhanced generalization, with equally good performance as achieved by the locally trained models.

### B. Assessment of Transferability to ANN

To allow for TL, we trained an ANN on the same training data compilations. This approach necessitated the preliminary process of hyperparameter tuning. We performed a bayesian optimization regarding the batch size, learning rate, weight decay factor, number of hidden layers, and the depth of the first hidden layer with roughly 100 configurations tested. Each hidden layer consists of a linear layer, an activation function, and batch normalization. The second and third hidden layer double in size, then each subsequent layer halves. The best hyperparameter configuration found is provided in Tab. II.

We carried out the same transferability analysis with the ANN as with the RF. The resulting RMSEs can be seen in the right part of Fig. 6. Overall, slightly worse RMSEs can be

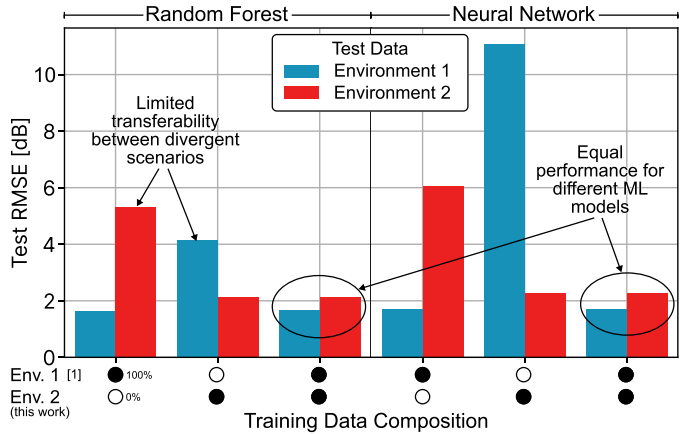


Fig. 6. Comparison of the generalizability of RF and ANN: RMSE on the test data for different training data compositions

observed with an exception when training on the new data and testing on the original data. The original data covers greater 3D distances between transmitter and receiver than new data (cf. Fig. 5). While this is not an issue with RFs, as they lack extrapolation capability, it is with ANNs, where in this particular case the deviation of  $y$  and  $\hat{y}$  increases together with the distance. However, the global model's performance is equally good compared to the RF making the ANN a suitable ML model alternative.

TABLE II  
CHOSEN HYPERPARAMETERS OF THE ANN.

Hyperparameter	Value
Batch size	1024
Learning rate	1e-4
Weight decay factor	5e-4
Activation function	Leaky ReLU
Hidden layer sizes	[512, 1024, 2048, 1024, 512, 256, 128, 64, 32]
Optimizer	Adam

### C. Exploiting the Trained Models for REM Generation

The trained ML models are subsequently used for generating area-covering REMs. In this process, the feature vector  $\mathbf{x}$  is derived for each REM cell (each receiver position of interest) and used for predicting  $\hat{y}$ . REMs for scenario G with BS position 7 are shown in Fig. 7. While the REM resolution for the predictions is solely limited by the computing resources, the resolution for the ground truth REM is constrained by the feasibility of carrying out high resolution measurements over a large area and the accuracy of the localisation. For the measured ground truth a REM cell resolution of 50 cm is used and for the predicted REM the resolution is set to 2.5 cm.

As already pointed out in the preceding section, both ML models demonstrate the capacity to accurately replicate the propagation effects. While a sample-wise comparison of this scenario produces an RMSE of 1.34 dB for the RF and 1.77 dB for the ANN, the resulting REMs appear pretty much identical for both methods with RMSEs of 1.53 dB and 1.60 dB, respectively, with only minor differences recognizable. In both REMs, the impact of obstacle-induced shadowing is distinctly observable, and a higher RSRP is evident in proximity to the

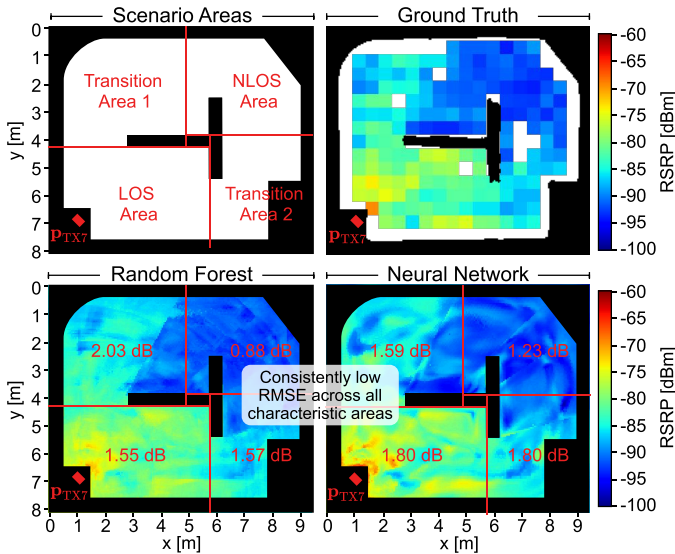


Fig. 7. Exemplary REM results: Measured ground truth at 50 cm and ML predictions for 2.5 cm cell resolution for scenario G with BS position 7. Additionally, the RMSE is shown for four different areas (red dB values).

BS, as is apparent from the measurements. However, the RF-based prediction exhibits some circular pattern with respect to the distance to the antenna, suggesting decision nodes influenced by the 3D distance between the transmitter and receiver. This behaviour is especially apparent in the vicinity of obstacles, thereby facilitating a clear differentiation between Line of Sight (LOS) and Non LOS (NLOS) conditions. Conversely, the REM generated by the ANN demonstrates a more continuous representation with fewer abrupt transitions. While obstacle-induced shadowing remains clearly identifiable, the ANN predicts lower RSRP values in the LOS region ahead of the obstacles compared to the RF model. For a better location-dependent comparison, we split the scenario into 4 areas: LOS, NLOS and Transition 1 and 2 (cf. Fig. 7 upper left). While the RF is moderately more accurate than the ANN for LOS and transition area 2, the latter produces significantly better predictions for transition area 1, while the RF is superior for the NLOS area.

#### D. Transmitter Placement

To identify the most suitable BS position, REMs are created for the first unseen scenarios of interest for each of the seven BS positions (see Fig. 4 scenario A) using the latest ML model. The ANN-generated REMs can be observed in Fig. 8. The mean highest RSRP is observed here for BS positions 1, 6, and 7 with position 6 having the lowest standard deviation. As expected, BS positions 3 to 5 exhibit the lowest mean RSRP

due to the presence of obstacles directly in front of the BS, leading to significant shadowing effects.

#### E. ML Model Adaptation Using Transfer Learning

Building on the preceding antenna placement, the network is subsequently deployed. In a realistic setting, network KPIs would be collected by communication participants, enabling further refinement of the propagation model. To simulate this process, we conducted a measurement run for the deployed network. Initially, we evaluated how accurately the models trained on [1] and scenarios A to H could predict the RSRP for the new, unseen scenarios. While the ML models achieve low RMSEs of approximately 2 dB on the already seen data, their performance degrades significantly in scenarios I to K, with RMSE values ranging from 3 to over 4 dB (cf. Fig. 10).

To enhance model performance in a new scenario, recently collected KPI values are leveraged to generate additional training samples. For further training of the ANN, we apply a learning rate of  $1e-5$  and train for additional 10 epochs. For proper comparison, both models are trained under identical hardware conditions, without multithreading or GPU acceleration. The results for scenario I are presented in Fig. 9.

Incorporating scenario I into training significantly reduces the RMSE for both models. While the RF requires all original training data (also referred to as source data), the ANN can adapt incrementally without using the source data and therefore offering advantages in terms of privacy preservation. This, however, comes at the expense of worse generalization, as the ANN exhibits a notably higher RMSE on the original dataset. Retaining source data for further training mitigates this issue but increases training time. To analyze this trade-off, we evaluate different proportions of source data: 100%, 50%, 20%, 10%, 1%, 0%. When incorporating only 10% of the source data in the TL approach, the ANN exhibits only a slight increase in RMSE on the source test data while achieving improved RMSE on scenario I and requiring less training time than the RF. Enabling GPU acceleration reduces the time from 56 to 3 s. Note that the training duration is strongly correlated with the number of training samples. With increasing amount of available data, the training time of the RF grows, whereas it remains unchanged for the TL approach.

In a realistic setting, the environment is constantly changing and new network KPIs emerge continuously, allowing further adaptation of the underlying ML model. We simulate this through the implementation of multiple TL iterations using the test scenarios I to K: Upon the modification of the environment, the network planning is initiated, followed by the

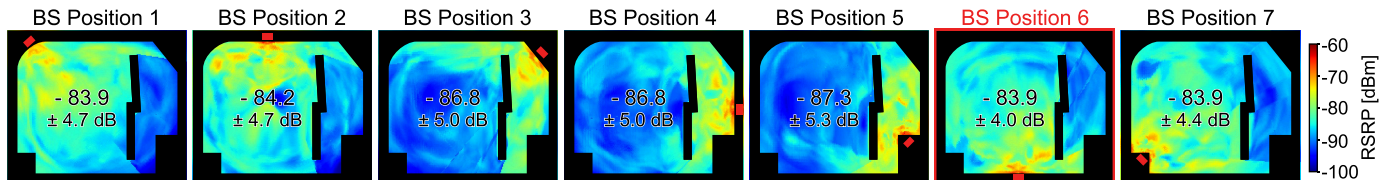


Fig. 8. Analysis of different BS locations: ANN-predicted REMs for scenario I and seven pre-selected BSs together with their mean RSRP and standard deviation. Identified best BS position is position 6.

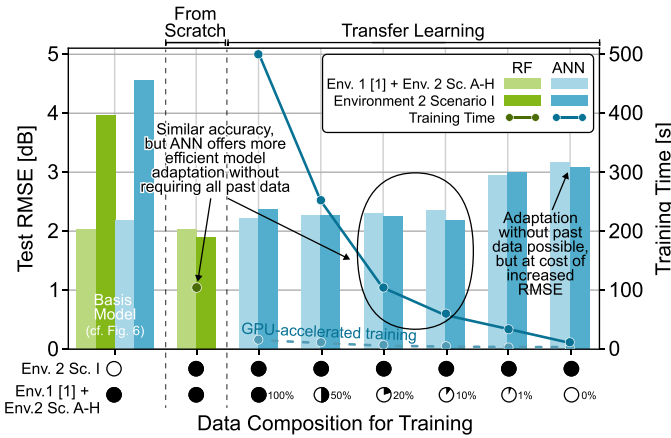


Fig. 9. Analyzing the trade-off between training time and accuracy: Test RMSE and training time for ML model adaption on scenario I

deployment of the network, KPI collection, and the utilization of the KPIs for adapting IndoorDRaGon’s ANN (cf. Fig. 2). The results on the test data can be seen in Fig. 10. With each TL iteration the model’s generalizability is improved with slightly increased RMSE for the already seen data but substantial improved RMSE for the scenario of interest. Additionally, it can be discerned that the first TL iteration not only reduces the test error on scenario I, but also for scenario J.

## VI. CONCLUSION AND OUTLOOK

In this paper we presented how the existing ML-based IndoorDRaGon channel model can be adapted to new environments. As demonstrated in our comprehensive performance evaluation the ML model requires training on data from the new environment to accurately perform RSRP predictions. As the RF utilized by the original IndoorDRaGon model [1] lacks continuous training capability, we examined ANNs as ML replacement. Although the latter demonstrates slightly poorer accuracy, it achieves notable strengths in the domains of rapid adaptation to novel scenarios and data privacy.

In this work, a rather simple network planning with only one BS was performed. Since the optimal solution here can be found by exhaustive search, we intend to extend the routine to multiple BSs and apply k-means clustering as used in [16] in future work. To enhance the generalizability of the proposed approach, we plan to include additional industrial hall environments in the future and benchmark IndoorDRaGon against other state-of-the-art ML techniques to thoroughly evaluate its performance. Another goal is to extend the IndoorDRaGon method to the mmWave frequency spectrum by applying TL. Future work will also explore federated learning for indoor environments to address privacy challenges in model transfer.

## ACKNOWLEDGMENT

This work has received funding by the German Federal Ministry of Research, Technology and Space (BMFTR) in the course of the 6GEM research hub under grant number 16KISK038. In addition, it has been supported by the Ministry of Economic Affairs, Innovation, Digitalisation and Energy of the State of North Rhine-Westphalia (MWIDE NRW) along with the Competence Center 5G.NRW under grant number 005-01903-0047.

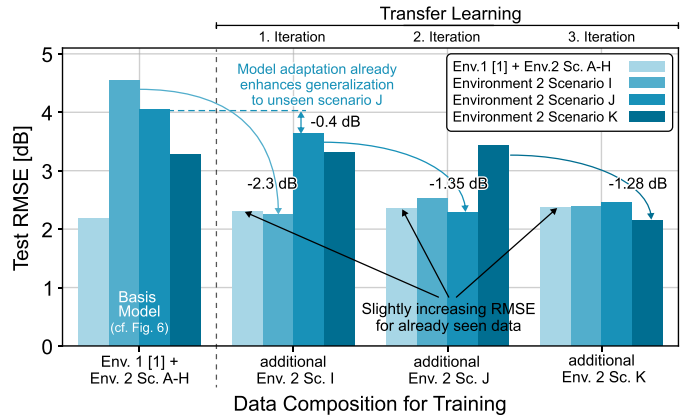


Fig. 10. Simulation of multiple environmental changes and model adjustments: ANN Test RMSE for multiple TL iterations

## REFERENCES

- [1] M. Geis, H. Schippers, M. Danger, C. Krieger, S. Böcker, J. Freytag, I. Priyanta, M. Roidl, and C. Wietfeld, “IndoorDRaGon: Data-Driven 3D Radio Propagation Modeling for Highly Dynamic 6G Environments,” in *Proc. European Wireless*, Oct 2023.
- [2] “3GPP TR 38.901 - Study on channel model for frequencies from 0.5 to 100 GHz, V 17.0.0,” 3GPP, Tech. Rep. 38.901, Apr 2022.
- [3] Z. Yun and M. F. Iskander, “Ray tracing for radio propagation modeling: Principles and applications,” *IEEE Access*, vol. 3, pp. 1089–1100, 2015.
- [4] S. Bakirtzis, I. Wassell, M. Fiore, and J. Zhang, “AI-Assisted Indoor Wireless Network Planning With Data-Driven Propagation Models,” *IEEE Network*, vol. 38, no. 6, pp. 451–458, 2024.
- [5] J. Thrane, B. Sliwa, C. Wietfeld, and H. Christiansen, “Deep Learning-based Signal Strength Prediction Using Geographical Images and Expert Knowledge,” in *Proc. IEEE GLOBECOM*, Taipei, Taiwan, Dec 2020.
- [6] A. Seretis and C. D. Sarris, “An Overview of Machine Learning Techniques for Radiowave Propagation Modeling,” *IEEE Trans. on Antennas and Propagation*, vol. 70, no. 6, pp. 3970–3985, 2022.
- [7] A. Seretis, C. Xu, and C. Sarris, “Fast Selection of Indoor Wireless Transmitter Locations With Generalizable Neural Network Propagation Models,” *IEEE Trans. on Antennas and Propagation*, vol. 72, no. 10, pp. 7927–7940, 2024.
- [8] S. Liu, T. Onishi, M. Taki, and S. Watanabe, “A Generalizable Indoor Propagation Model Based on Graph Neural Networks,” *IEEE Trans. on Antennas and Propagation*, vol. 71, no. 7, pp. 6098–6110, 2023.
- [9] M. T. Waheed, Y. Fahmy, and A. Khattab, “DeepChannel: Robust Multimodal Outdoor Channel Model Prediction in LTE Networks Using Deep Learning,” *IEEE Access*, vol. 10, pp. 79 289–79 300, 2022.
- [10] R. Jaiswal, M. Elnourani, S. Deshmukh, and B. Beferull-Lozano, “Deep Transfer Learning Based Radio Map Estimation for Indoor Wireless Communications,” in *Proc. IEEE International Workshop on Signal Processing Advances in Wireless Communication (SPAWC)*, 2022.
- [11] S. Bakirtzis, J. Chen, K. Qiu, J. Zhang, and I. Wassell, “EM DeepRay: An Expedient, Generalizable, and Realistic Data-Driven Indoor Propagation Model,” *IEEE Trans. on Antennas and Propagation*, vol. 70, no. 6, pp. 4140–4154, 2022.
- [12] T. Nagao and T. Hayashi, “Fine-Tuning for Propagation Modeling of Different Frequencies with Few Data,” in *Proc. IEEE VTC-Fall*, Sep 2022.
- [13] K. Mei, J. Liu, X. Zhang, K. Cao, N. Rajatheva, and J. Wei, “A Low Complexity Learning-Based Channel Estimation for OFDM Systems With Online Training,” *IEEE Trans. on Communications*, vol. 69, no. 10, pp. 6722–6733, 2021.
- [14] L. Clark, J. A. Edlund, M. S. Net, T. S. Vaquero, and A. akbar Agha-Mohammadi, “PropEM-L: Radio Propagation Environment Modeling and Learning for Communication-Aware Multi-Robot Exploration,” in *Robotics: Science and Systems 2022*, Jul 2022.
- [15] S. Macenski, F. Martín, R. White, and J. G. Clavero, “The Marathon 2: A Navigation System,” in *2020 IEEE/RSJ International Conference on Intelligent Robots and Systems (IROS)*, 2020, pp. 2718–2725.
- [16] C. Bektas, S. Böcker, B. Sliwa, and C. Wietfeld, “Rapid Network Planning of Temporary Private 5G Networks with Unsupervised Machine Learning,” in *Proc. IEEE VTC-Fall*, Sep 2021.